

Orbit and Sinus Classification Based on Force Histogram Computation

Pascal Matsakis
CECS Dept.,
Missouri-Columbia Univ.,
Columbia, MO 65211, USA

Laurent Wendling
LORIA, BP 239,
54 506 Vandoeuvre Cedex,
France

Abstract

In a previous work, we defined a new approach to evaluating directional relations between objects (such as “is to the right of”, “is above”...). The approach is based on the computation of a histogram of forces. We show in the present paper that the notion of the histogram of forces can also be useful in pattern recognition. The aim of this study is to classify orbits and sinuses. Using force histograms instead of geometrical criteria (like compactness or degree of ellipticity) allows more accurate classification to be produced. Moreover, the proposed approach is low computing time.

1. Introduction

The database used in this study is composed of several orbit and sinus drawings provided by a French medicine team (Université Paul Sabatier). These drawings were defined from craniums (3rd century A.D.) found in a necropolis (Nubia [6]). Experts distinguish four models of sinuses (bean, foliaceous, pyramidal, fan-shaped) and four models of orbits (rectangular, elliptical, trapezoid, circular) [4]. Our aim is to classify each orbit and sinus of the database. In the same drawing the two orbits belong to the same class whereas the two sinuses are independent.

2. Relevant Features

2.1. Classical Features

In a first approach, simple geometrical characteristics were used to classify the objects: the degree of compactness, and the degree of ellipticity (the axes being given by the moments of order 0 to 2 [5]). Nevertheless, these features (and their combination) often gave incoherent results. The perimeter has a large effect on the calculation of the compactness, and when the drawing is not sharp, the use of

such a feature may end in a bad classification (for instance, the orbits in example 1 were found elliptical instead of rectangular). A polygonal approximation of the objects should be a solution to this problem. However, the loss of information may result in a low recognition rate for the fan-shaped sinuses. The degree of ellipticity is not suited either to the classification of this type of object. An original approach based on the computation of a histogram of forces is presented in the next section.

2.2. Histograms of Forces

A histogram of forces provides a representation of the relative position of an object with regard to another, and allows rapid fuzzy qualitative evaluation of any directional relationship between these objects [2] [3]. In this section, we briefly explain how such a histogram is computed. The euclidean affine plane is referred to the directional orthogonal frame (O, \vec{i}, \vec{j}) . Let θ and v be two reals, \vec{i}_θ and \vec{j}_θ the respective images of \vec{i} and \vec{j} by θ -angle rotation, and $\Delta_\theta(v)$ the oriented line whose frame of reference is defined by the vector \vec{i}_θ and the point of coordinates $(0, v)$ – relative to $(O, \vec{i}_\theta, \vec{j}_\theta)$. T denotes be the set of triples $(\theta, A_\theta(v), B_\theta(v))$, where θ and v describe \mathbb{R} and A and B describe the set of objects of the plane. $A_\theta(v)$ is a longitudinal section of A : $A_\theta(v) = A \cap \Delta_\theta(v)$. Likewise: $B_\theta(v) = B \cap \Delta_\theta(v)$.

2.2.1 Handling of Couples of Segments

Let φ be a map from \mathbb{R} into \mathbb{R}_+ , null on \mathbb{R}_- , and continuous on \mathbb{R}_+^* . The following function is termed the *function generated by φ* .

$$f \left| \begin{array}{l} \mathbb{R}_+ \times \mathbb{R} \times \mathbb{R}_+ \rightarrow \mathbb{R}_+ \\ (x, y, z) \mapsto \int_{y+z}^{x+y+z} \left(\int_0^z \varphi(u-v) dv \right) du \end{array} \right.$$

Now, let A and B be two objects, θ and v two real numbers, I one of the segments that form $A_\theta(v)$, and J one of the segments that form $B_\theta(v)$. The relative position between I and J is defined by a triple (d_I, D_{IJ}^0, d_J) of real numbers (Fig. 1). We consider (I, J) an argument put

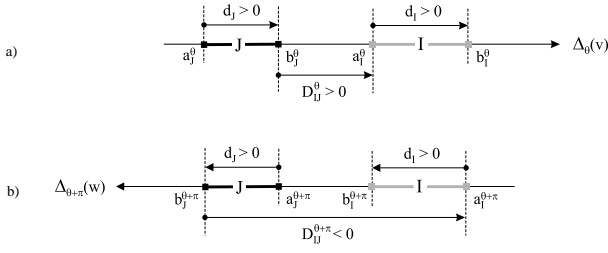


Figure 1. Couple of segments.

forward to support the proposition “A is in direction θ of B”. The value $f(d_I, D_{IJ}^\theta, d_J)$ represents the weight of this argument:

$$\begin{aligned} f(d_I, D_{IJ}^\theta, d_J) &= \int_{a_I^\theta}^{b_I^\theta} \left(\int_{a_J^\theta}^{b_J^\theta} \varphi(u-v) .dv \right) .du \\ &= \int_{a_J^\theta}^{b_J^\theta} \left(\int_{a_I^\theta}^{b_I^\theta} \varphi(u-v) .du \right) .dv \\ &= \int_{D_{IJ}^\theta + d_I}^{d_I + D_{IJ}^\theta + d_J} \left(\int_0^{d_J} \varphi(u-v) .dv \right) .du \end{aligned}$$

2.2.2 Handling of Longitudinal Sections

The handling of couples of longitudinal sections is carried out by way of a function F from T to \mathbb{R}_+ . Let A and B be two objects and θ and v two reals. There exists one set $\{I_i\}_{i \in 1..n}$ of mutually disjoint segments, and only one, such that: $A_\theta(v) = \cup_{i \in 1..n} I_i$. Likewise, there exists one set $\{J_j\}_{j \in 1..m}$ of segments such that: $B_\theta(v) = \cup_{j \in 1..m} J_j$.

We consider the $(A_\theta(v), B_\theta(v))$ couple an argument put forward to support the proposition “A is in direction θ of B”. The weight of this argument is represented by $F(\theta, A_\theta(v), B_\theta(v))$. It is computed by summing the weights $f(d_I, D_{IJ}^\theta, d_J)$ of the (I, J) arguments, where I and J describe $\{I_i\}_{i \in 1..n}$ and $\{J_j\}_{j \in 1..m}$ respectively (Fig. 2):

$$F(\theta, A_\theta(v), B_\theta(v)) = \sum_{i \in 1..n} \sum_{j \in 1..m} f(d_{I_i}, D_{I_i J_j}^\theta, d_{J_j})$$

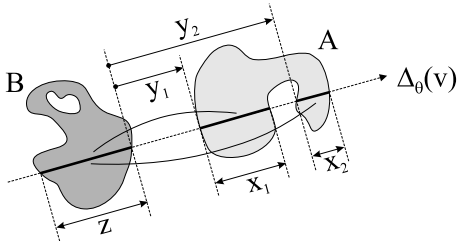


Figure 2. $F(\theta, A_\theta(v), B_\theta(v)) = f(x_1, y_1, z) + f(x_2, y_2, z)$

2.2.3 Handling of Directions

For any function F from T into \mathbb{R}_+ and for any couple (A, B) of objects, let us denote by F^{AB} the function de-

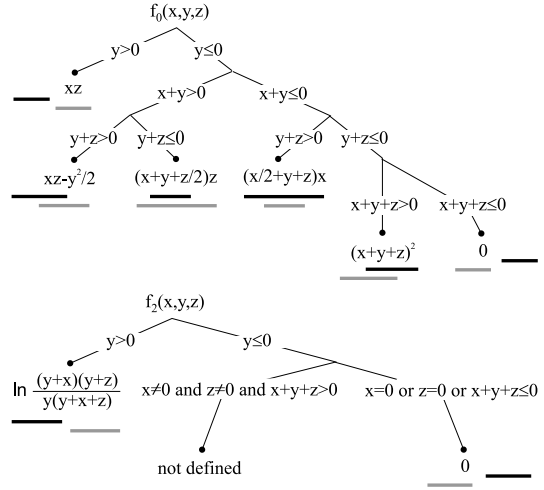


Figure 3. Functions f_0 and f_2

finied by:

$$\begin{aligned} F^{AB} | \quad & \mathbf{R} \rightarrow \mathbf{R}_+, \\ & \theta \mapsto \int_{-\infty}^{+\infty} F(\theta, A_\theta(v), B_\theta(v)) .dv \end{aligned}$$

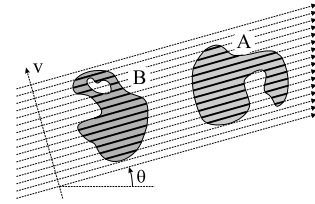
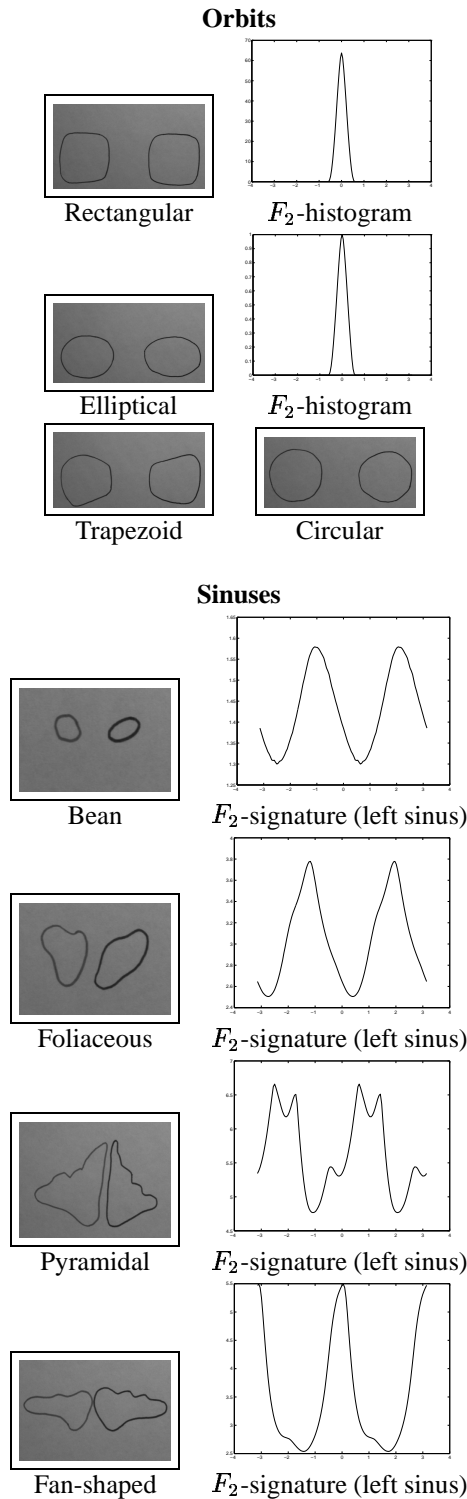


Figure 4. $F^{AB}(\theta) = \int_{-\infty}^{+\infty} F(\theta, A_\theta(v), B_\theta(v)) .dv$

If F^{AB} is defined on \mathbb{R} , and F is defined at $(\theta, A_\theta(v), B_\theta(v))$ for any couple (θ, v) of reals, the couple (A, B) is termed F -assessable. $F^{AB}(\theta)$ then represents the total weight of the arguments stated in favor of the proposition “A is in direction θ of B”. For any real number r , let φ_r be the map from \mathbb{R} into \mathbb{R}_+ , null on \mathbb{R}_- , such that: $\forall d \in \mathbb{R}_+, \varphi_r(d) = 1/d^r$. Let f_r be the function generated by φ_r and F_r the one generated by f_r . F_0^{AB} and F_2^{AB} have very different and very interesting characteristics. F_0^{AB} is fundamentally equivalent to the histogram of angles \mathcal{A}^{AB} [1] (even though the first histogram arises from the continuous case and the second from the discrete case). Assuming that each object is a homogeneous material surface of unit specific mass, $F_2^{AB}(\theta)$ represents the scalar resultant of elementary forces of gravity: the forces exerted by the A points on those of B , each tending to move B in direction θ . That is why function F^{AB} is called the histogram of forces associated with (A, B) (via F). The expressions of f_0 and f_2 are shown in Figure 3. For these functions, a couple of aligned segments is seen as a triple (x, y, z) of real numbers: x denotes the length of the referent segment (black

line), z the length of the argument segment (gray line). The algebraic expression corresponding to the process of a given couple depends on the relative position of the segments.

3 Prototypes

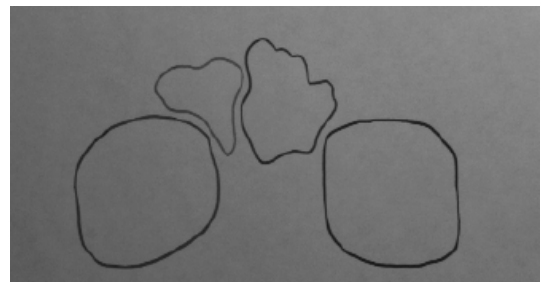


Eight drawings defined by an expert constituted the prototypes of the classes of orbits and sinuses. Each drawing was scanned, the resulting images were filtered, and the full regions corresponding to the orbits and sinuses were determined and labelled. Then 24 histograms were computed. Half are histograms of constant forces, denoted F_0 . They result from function f_0 . The others, F_2 , are histograms of gravitational forces. They result from function f_2 . Each histogram represents the relative position (i) of the right orbit with regard to the left one (ii) or of the right sinus with regard to itself (iii) or of the left sinus with regard to itself. In the second and third cases, the histogram actually corresponds to a “signature” of the sinus.

4 Experimental results

About forty drawings of orbits and sinuses – defined from craniums found in a necropolis – constituted the test database. Each drawing was scanned and the resulting image processed as above. Then, for each image, six histograms were computed (F_0 and F_2 , for the couple of orbits, and for each sinus). The classification of orbits and sinuses is based on the computation of similarities between the histograms associated with the test images and those associated with the prototypes. We used the following ratio, where A and B are the histograms to compare: $R = 100 \times \frac{|A \cap B|}{|A \cup B|}$. Three results are presented below. The following symbols are used for the orbits: Re = Rectangular, El = Elliptical, Tr = Trapezoid, Ci = Circular and for the sinuses: Be = Bean, Fo = Foliaceous, Py = Pyramidal, Fs = Fan-shaped.

Example 1



• Similarity ratios (F_0)

Orbits		Sinus	left	right
Re	94.90	Be	22.05	11.67
El	85.89	Fo	92.32	37.90
Tr	89.60	Py	85.62	80.74
Ci	93.52	Fs	59.07	38.42

- Similarity ratios (F_0 normalized)

Orbits		Sinus	left	right
Re	96.51	Be	65.62	39.07
El	79.39	Fo	92.32	66.40
Tr	87.88	Py	82.14	72.90
Ci	92.53	Fs	56.48	33.63

- Similarity ratios (F_2)

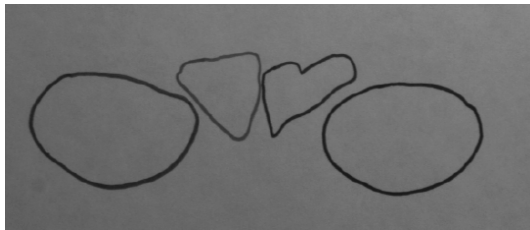
Orbits		Sinus	left	right
Re	97.49	Be	7.59	1.37
El	82.68	Fo	61.32	11.09
Tr	78.96	Py	89.68	37.33
Ci	95.30	Fs	57.57	10.41

- Similarity ratios (F_2 normalized)

Orbits		Sinus	left	right
Re	96.51	Be	59.31	37.29
El	83.00	Fo	95.20	62.23
Tr	88.10	Py	90.36	78.20
Ci	93.33	Fs	68.99	43.27

The size of the sinuses may vary a lot from one cranium to the other, and numerous misclassifications happen if the histograms are not normalized. In this first example, the left sinus is actually foliaceous, and not pyramidal.

Example 2



- Similarity ratios (F_0 normalized)

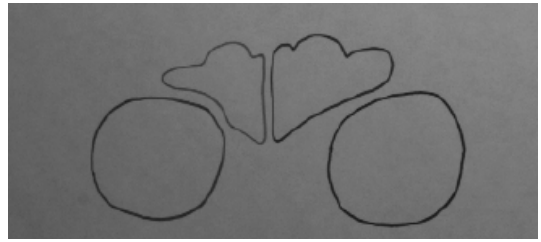
Orbits		Sinus	left	right
Re	62.87	Be	67.86	91.13
El	76.07	Fo	96.40	73.30
Tr	68.92	Py	79.43	58.42
Ci	65.75	Fs	58.41	79.32

- Similarity ratios (F_2 normalized)

Orbits		Sinus	left	right
Re	53.55	Be	63.31	81.46
El	74.14	Fo	94.29	81.43
Tr	70.09	Py	84.66	65.79
Ci	66.20	Fs	73.65	93.57

Even normalized, the F_0 -histograms often lead to incorrect classifications. In this second example, the right sinus is actually fan-shaped, and not bean-shaped.

Example 3



- Similarity ratios (F_2 normalized)

Orbits		Sinus	left	right
Re	90.21	Be	51.42	55.82
El	92.93	Fo	86.11	93.36
Tr	96.52	Py	95.87	95.67
Ci	94.14	Fs	59.82	64.94

The use of normalized F_2 -histograms allows most of the tested objects to be classified correctly. However, some particular cases have to be pointed out. The two orbits of a cranium normally belongs to the same class (whereas the two sinuses are independent and may belong to different classes), but there are a few exceptions. In this third example for instance, the experts consider the left orbit circular and the right one trapezoid. We found three similar cases in the database.

5 Conclusion

We have shown in this paper that the notion of the histogram of forces can be exploited in pattern recognition. This has been illustrated with a classification problem. The notion of the F -signature has also been introduced. The F -signature of an object is a powerful representation of its shape.

References

- [1] A. R. K. Miyajima. Spatial organization in 2d segmented images: Representation and recognition of primitive spatial relations. *Fuzzy Sets and Systems*, 65(2/3):225–236, 1994.
- [2] P. Matsakis and L. Wendling. A new way to represent the relative position between areal objects. *IEEE PAMI*, 21(7):634–643, 1999.
- [3] P. Matsakis, L. Wendling, and J. Desachy. Représentation de la position relative d'objets 2d au moyen d'un histogramme de forces. *Traitement du Signal*, 15(1):25–38, 1998.
- [4] J. Szilvassy. Zur variation, entwicklung und vererbung der stirnhohlen. *Ann. Naturhist. mus. Wien.*, pages 97–125, 1982.
- [5] R. Teag. Image analysis via the general theory of moments. *Optical Society of America*, 70(8):920–921, 1980.
- [6] A. Vila. *La prospection archéologique de la vallée du Nil au sud de la cataracte de Dal*. 1994.